

2

OFFICE OF NAVAL RESEARCH

Grant N00014-90-J-1193

TECHNICAL REPORT No. 41

DTIC FILE COPY

AD-A231 327

Critical Behavior in Magnetic Superlattices

by

T. Hai, Z. Y. Li, D. L. Lin and Thomas F. George

Prepared for publication

in

Journal of Magnetism and Magnetic Materials

Departments of Chemistry and Physics
State University of New York at Buffalo
Buffalo, New York 14260

DTIC
ELECTE
JAN 30 1991
S D D

January 1991

Reproduction in whole or in part is permitted for any purpose of the United States Government.

This document has been approved for public release and sale; its distribution is unlimited.

91 1 29 010

REPORT DOCUMENTATION PAGE

Form Approved
OMB No. 0704-0188

1a. REPORT SECURITY CLASSIFICATION Unclassified		1b. RESTRICTIVE MARKINGS	
2a. SECURITY CLASSIFICATION AUTHORITY		3. DISTRIBUTION/AVAILABILITY OF REPORT Approved for public release; distribution unlimited	
2b. DECLASSIFICATION/DOWNGRADING SCHEDULE		4. PERFORMING ORGANIZATION REPORT NUMBER(S) UBUFFALO/DC/91/TR-41	
4. PERFORMING ORGANIZATION REPORT NUMBER(S) UBUFFALO/DC/91/TR-41		5. MONITORING ORGANIZATION REPORT NUMBER(S)	
6a. NAME OF PERFORMING ORGANIZATION Depts. Chemistry & Physics State University of New York	6b. OFFICE SYMBOL (if applicable)	7a. NAME OF MONITORING ORGANIZATION	
6c. ADDRESS (City, State, and ZIP Code) Fronczak Hall, Amherst Campus Buffalo, New York 14260		7b. ADDRESS (City, State, and ZIP Code) Chemistry Program 800 N. Quincy Street Arlington, Virginia 22217	
8a. NAME OF FUNDING/SPONSORING ORGANIZATION Office of Naval Research	8b. OFFICE SYMBOL (if applicable)	9. PROCUREMENT INSTRUMENT IDENTIFICATION NUMBER Grant N00014-90-J-1193	
8c. ADDRESS (City, State, and ZIP Code) Chemistry Program 800 N. Quincy Street Arlington, Virginia 22217		10. SOURCE OF FUNDING NUMBERS	
		PROGRAM ELEMENT NO.	PROJECT NO.
		TASK NO.	WORK UNIT ACCESSION NO.
11. TITLE (Include Security Classification) Critical Behavior in Magnetic Superlattices			
12. PERSONAL AUTHOR(S) T. Hai, Z. Y. Li, D. L. Lin and Thomas F. George			
13a. TYPE OF REPORT	13b. TIME COVERED FROM _____ TO _____	14. DATE OF REPORT (Year, Month, Day) January 1991	15. PAGE COUNT 20
16. SUPPLEMENTARY NOTATION Prepared for publication in the <i>Journal of Magnetism and Magnetic Materials</i>			
17. COSATI CODES		18. SUBJECT TERMS (Continue on reverse if necessary and identify by block number)	
FIELD	GROUP	SUB-GROUP	
			CRITICAL BEHAVIOR
			MAGNETIC SUPERLATTICES,
			EFFECTIVE FIELD THEORY,
			CORRELATIONS
			TWO FERROMAGNETS
			CUBIC ISING MODEL
19. ABSTRACT (Continue on reverse if necessary and identify by block number)			
<p>Based on the effective field theory with correlations, the critical behavior of a magnetic superlattice consisting of two different ferromagnets is examined. A simple cubic Ising model with nearest-neighbor coupling is assumed. It is found that there exists a critical value for the interface exchange coupling above which the interface magnetism appears. The critical temperature of the superlattice is studied as a function of the thickness of the constituents in a unit cell and of the exchange coupling energies in each material. A phase diagram is also given.</p>			
20. DISTRIBUTION/AVAILABILITY OF ABSTRACT <input checked="" type="checkbox"/> UNCLASSIFIED/UNLIMITED <input checked="" type="checkbox"/> SAME AS RPT. <input type="checkbox"/> DTIC USERS		21. ABSTRACT SECURITY CLASSIFICATION Unclassified	
22a. NAME OF RESPONSIBLE INDIVIDUAL Dr. David L. Nelson		22b. TELEPHONE (Include Area Code) (202) 696-4410	22c. OFFICE SYMBOL

Critical behavior in magnetic superlattices

T. Hai
P. O. Box 1001-73
Zhengzhou 450002, P. R. China

Z. Y. Li*, D. L. Lin and Thomas F. George
Department of Physics and Astronomy
State University of New York at Buffalo
Buffalo, New York 14260, USA

Abstract

Based on the effective field theory with correlations, the critical behavior of a magnetic superlattice consisting of two different ferromagnets is examined. A simple cubic Ising model with nearest-neighbor coupling is assumed. It is found that there exists a critical value for the interface exchange coupling above which the interface magnetism appears. The critical temperature of the superlattice is studied as a function of the thickness of the constituents in a unit cell and of the exchange coupling energies in each material. A phase diagram is also given.

* On leave of absence from the Department of Physics, Suzhou University,
Suzhou 215006, P. R. China



Accession For	
NTIS	<input checked="" type="checkbox"/>
CR&I	<input checked="" type="checkbox"/>
DTIC	<input type="checkbox"/>
TAB	<input type="checkbox"/>
Unannounced	<input type="checkbox"/>
Justification	
By	
Distribution/	
Availability Codes	
Dist	Avail and/or Special
A-1	

I. Introduction

In recent years, there has been increasing interest in the nature of spin waves as well as critical phenomena in various magnetic layered structures and superlattices. Ma and Tsai¹ have studied the variation with modulation wavelength of the Curie temperature for a Heisenberg magnetic superlattice. Their results agree qualitatively with experiments on the Cu/Ni film.² Superlattice structures composed of alternating ferromagnetic and antiferromagnetic layers have been investigated by Hinchey and Mills,^{3,4} using a localized spin model. A sequence of spin-reorientation transitions are found to be different for superlattices with the antiferromagnetic component consisting of an even or odd number of spin layers. In addition, the spin-wave spectrum and infrared absorption spectrum are calculated.

For a periodic multilayer system formed from two different ferromagnetic materials, Fishman et al⁵ have discussed its statics and dynamics within the framework of the Ginzburg-Landau formulation. They have computed the transition temperature and spin-wave spectra. On the other hand, the Landau formalism of Camley and Tilley⁶ has been applied to calculate the critical temperature in the same system.⁷ Compared to Ref. 5, the formalism of Ref. 6 appears to be more general because it allows for a wider range of boundary conditions and includes the sign of exchange coupling across the interface.

For more complicated superlattices with arbitrary number of different layers in an elementary unit, Barnas⁸ has derived some general dispersion equations for the bulk and surface magnetic polaritons. These equations are then applied to magnetostatic modes and to retarded wave propagation in the Voigt geometry.⁹

We study, in this article, the critical temperature in an infinite superlattice consisting of two ferromagnetic materials with different bulk

properties. In particular, we consider the two constituents A and B with different bulk transition temperatures as a simple model, i.e., $T_c^{(a)} \neq T_c^{(b)}$. The interface is in general different in nature from both bulks, even if the bulk critical temperatures are the same. We use the effective-field theory with correlations¹⁰ in the present work, as it is believed to be far superior to the standard mean-field approximation.

Because of the periodicity of the superlattice structure, we restrict our discussions to a unit cell which interacts with its nearest-neighbor cells via interface couplings. Thus the system can be treated by extending the method developed for a magnetic slab.¹¹ Our major concerns are the dependence of the transition temperature on the thickness of individual constituents in the cell and the influence of the interface magnetic properties on the phase transition temperature. These questions, to our knowledge, have not been considered in the literature thus far.

In Sec. II, we outline the theory and derive the equation that determines the transition temperature. Numerical results are discussed in Sec. III where the existence of the interface magnetic phase transition is discovered and the critical value of the interface coupling relative the bulk coupling is determined. A brief conclusion is given in Sec. IV.

II. Theory

Consider an infinite superlattice consisting of two different ferromagnetic materials A and B. For simplicity, we restrict our attention to the case of simple cubic Ising-type structures. The periodic condition suggests that we only have to consider one unit cell which interacts with its nearest neighbors via the interface coupling. The situation is depicted in Fig. 1. The coupling strength between nearest-neighbor spins in A(B) is

denoted by $J_a(J_b)$, while J_{ab} stands for the exchange coupling between the nearest-neighbor spins across the interface. The corresponding number of atomic layers in A(B) is $L_a(L_b)$, and the thickness of the cell is $L = L_a + L_b$. The Hamiltonian of the system is given by

$$H = - \frac{1}{2} \sum_{i,j} J_{ij} S_i S_j \quad , \quad (1)$$

where the sum is taken over all the nearest-neighbor pairs only once, $S_i = \pm 1$ is the usual Ising variable, and J_{ij} stands for one of the three coupling constants depending on where the spin pair is located.

To evaluate the mean spin $\langle S_i \rangle$, we start with the exact Callen identity,¹²

$$\langle S_i \rangle = \langle \tanh \left(\beta \sum_j J_{ij} S_j \right) \rangle \quad , \quad (2)$$

where $\beta = 1/k_B T$, $\langle \dots \rangle$ indicates the usual canonical ensemble average for a given configuration of $\{J_{ij}\}$, and j runs over all nearest neighbors of site i . We now introduce the differential operator $D = \frac{\partial}{\partial x}$ and recall that the displacement operator $\exp(\alpha D)$ satisfies the relation

$$\exp(\alpha D) f(x) = f(x+\alpha) \quad . \quad (3)$$

Equation (2) can then be rewritten, with the help of (3), as

$$\langle S_i \rangle = \langle \exp(D \sum_j J_{ij} S_j) \rangle [\tanh(\beta x)]_{x=0}$$

$$= \langle \prod_j [\cosh(DJ_{ij}) + S_j \sinh(DJ_{ij})] \rangle \tanh(\beta x) \Big|_{x=0} \quad (4)$$

This equation represents a set of L coupled equations for the L spin layers in the unit cell. Each layer is only coupled to its nearest-neighbor layers. The multi-spin correlation function, however, must be decoupled before a practical calculation can be made. We follow the standard procedure¹³ with the decoupling approximation $\langle x_1 x_2 \dots x_\ell \rangle = \langle x_1 \rangle \langle x_2 \rangle \dots \langle x_\ell \rangle$. Thus the average atomic magnetization of each layer is given by

$$m_1 = [\cosh(DJ_{ab}) + m_0 \sinh(DJ_{ab})][\cosh(DJ_a) + m_1 \sinh(DJ_a)]^4 \\ \times [\cosh(DJ_a) + m_2 \sinh(DJ_a)] f(x) \Big|_{x=0} \quad (5a)$$

$$\vdots$$

$$m_i = [\cosh(DJ_a) + m_{i-1} \sinh(DJ_a)][\cosh(DJ_a) + m_i \sinh(DJ_a)]^4 \\ \times [\cosh(DJ_a) + m_{i+1} \sinh(DJ_a)] f(x) \Big|_{x=0} \quad 2 \leq i \leq L_a \quad (5b)$$

$$\vdots$$

$$m_{L_a} = [\cosh(DJ_a) + m_{L_a-1} \sinh(DJ_a)][\cosh(DJ_a) + m_{L_a} \sinh(DJ_a)]^4 \\ \times [\cosh(DJ_{ab}) + m_{L_a+1} \sinh(DJ_{ab})] f(x) \Big|_{x=0} \quad (5c)$$

$$m_{L_a+1} = [\cosh(DJ_{ab}) + m_{L_a} \sinh(DJ_{ab})][\cosh(DJ_b) + m_{L_a+1} \sinh(DJ_b)]^4 \\ \times [\cosh(DJ_b) + m_{L_a+2} \sinh(DJ_{ab})] f(x) \Big|_{x=0} \quad (5d)$$

$$\vdots$$

$$\begin{aligned}
m_j &= [\cosh(DJ_a) + m_{j-1} \sinh(DJ_b)] [\cosh(DJ_b) + m_j \sinh(DJ_b)]^4 \\
&\quad [\cosh(DJ_b) + m_{j+1} \sinh(DJ_b)] f(x) \Big|_{x=0} \quad L_a \leq j \leq L-1 \quad (5e) \\
&\quad \vdots \\
m_L &= [\cosh(DJ_b) + m_{L-1} \sinh(DJ_b)] [\cosh(DJ_b) + m_L \sinh(DJ_b)]^4
\end{aligned}$$

$$[\cosh(DJ_{ab}) + m_{L+1} \sinh(DJ_{ab})] f(x) \Big|_{x=0} \quad (5f)$$

where we have defined

$$f(x) = \tanh(\beta x) \quad (6)$$

on which the operator D applies. The variable x is set to zero at the end of the calculation in each equation. It is observed that the periodic condition of the superlattice is indeed satisfied, namely, $m_0 = m_L$ and $m_1 = m_{L+1}$. As the temperature becomes higher than the critical temperature, the whole system becomes demagnetized. Thus, we can determine T_c from Eq. (5) by requiring that the mean atomic magnetization in every spin layer approaches zero. Consequently, all terms of the order higher than linear in Eqs. (5) can be neglected. This leads to a set of simultaneous equations

$$\begin{aligned}
(1-4A_1)m_1 - A_2m_0 - A_1m_2 &= 0 \\
&\vdots \\
(1-4A_3)m_1 - A_3(m_{1-1} + m_{1+1}) &= 0 \\
&\vdots \\
(1-4A_1)m_{L_a} - A_1m_{L_a-1} - A_2m_{L_a+1} &= 0
\end{aligned}$$

$$\begin{aligned}
& \vdots \\
& (1-4A_4)^{m_{L_a+1}} - A_5^{m_{L_a}} - A_4^{m_{L_a+2}} = 0 \\
& \vdots \\
& (1-4A_6)^{m_j} - A_6^{(m_j-1-m_{j+1})} = 0 \\
& \vdots \\
& (1-4A_4)^{m_L} - A_4^{m_{L-1}} - A_5^{m_{L+1}} = 0 \quad ,
\end{aligned} \tag{7}$$

where the coefficients are given by

$$\begin{aligned}
A_1 &= \cosh^4(DJ_a) \sinh(DJ_a) \cosh(DJ_{ab}) f(x) \Big|_{x=0} \\
A_2 &= \cosh^5(DJ_a) \sinh(DJ_{ab}) f(x) \Big|_{x=0} \\
A_3 &= \cosh^5(DJ_a) \sinh(DJ_a) f(x) \Big|_{x=0} \\
A_4 &= \cosh^4(DJ_b) \sinh(DJ_b) \cosh(DJ_{ab}) f(x) \Big|_{x=0} \\
A_5 &= \cosh^5(DJ_b) \sinh(DJ_{ab}) f(x) \Big|_{x=0} \\
A_6 &= \cosh^5(DJ_b) \sinh(DJ_b) f(x) \Big|_{x=0} \quad .
\end{aligned} \tag{8}$$

The secular equation of this set of coupled equations is

Fig. 1. Four cases of different L_a values are plotted for fixed J_a and J_{ab} . We first note that T_c decreases with increasing L_a , in general. This is because we have assumed $J_a < J_b$ in our calculation, and it is well known that the bulk transition temperature is approximately proportional to the exchange coupling if the spin and lattice structure are specified. For a given L_a , it is observed that T_c increases steadily as L increases indefinitely. All the curves approach the same limiting value $T_c = 5.073 J_b/k_B$, which is simply $T_c^{(b)}$. This is of course easily understood.

To study the effects of the interface exchange coupling on the transition temperature of the superlattice, T_c is calculated for various J_{ab} but fixed J_a and L_a . Figure 3 shows the results for $J_a = J_b$. Curve c corresponds to the case $J_{ab} = J_b$ and appears like that of a slab of material B. It is very interesting to see that there exists a critical interface coupling $J_{ab}^c = 1.46 J_b$ such that T_c remains constant for any L_b , as represented by curve b. For J_{ab}^c larger than this critical value, we find that T_c is higher than both $T_c^{(a)}$ and $T_c^{(b)}$. Curve a illustrates one such particular case $J_{ab} = 2J_b$. This suggests that there exists an interface magnetism in the system. For $J_{ab} > J_{ab}^c$, the system may order in the interface layers before it orders in other layers. The situation does not change for $J_a \neq J_b$. The results for $J_a = 0.5 J_b$ are plotted in Fig. 4, whose curves are very similar except that the critical interface coupling J_{ab}^c in this case is bigger than in Fig. 3. This is because the lower $T_c^{(a)}$ needs a stronger, compensating interface exchange coupling in order to reach the interface phase transition.

Figure 5 demonstrates that as long as $J_a = J_b$, the critical coupling $J_{ab}^c = 1.46 J_b$ does not depend upon the thickness L_a . Curve d remains the same for all three cases calculated, while for $J_{ab} = 2.0 J_b$ and $0.1 J_b$, T_c behaves very differently when L_a is varied. Curves (a,a'), (b,b') and (c,c') correspond to

$L_a = 3, 5$ and 10 respectively. For $J_{ab} > J_{ab}^c$ when the interface magnetism appears, T_c decreases as L increases. For the a and b cases, material B dominates the system for $L > 13$. For the case c, $L_a \sim 10$, and T_c drops quickly at the beginning and approaches $T_c^{(b)}$ for $L \geq 20$. On the other hand, the transition temperature increases with L for $J_{ab} < J_{ab}^c$. The apparently anomalous behavior of curve c' can be understood in the following manner. As $J_{ab} = 0.1 J_b$, T_c is mainly determined by material A(B) if $L_a(L_b)$ is larger than $L_b(L_a)$. Hence, T_c changes little until L approaches 18 , because $L_a = 10$ in this case.

Figure 6 shows the phase diagram of the system by plotting the critical interface exchange coupling as a function of J_a . Three different thicknesses L_a are plotted. It is interesting to note that the three curves meet when $J_a = J_b$, suggesting that the critical interface exchange is independent of the relative thickness of the constituents in the unit cell as long as their exchange couplings are the same. This is of course in agreement with the above results in Fig. 5.

We have considered ferromagnetic interface coupling in our discussion. The critical temperature of the system, however, remains the same if the interface exchange coupling becomes antiferromagnetic. This is consistent with the discussion in Ref. 7.

IV. Conclusions

We have investigated the criticality of a two-component ferromagnetic superlattice by considering one unit cell, assuming nearest-neighbor spin exchange couplings. The interface exchange energy is, in general, different from either of the bulk ones. For the first time, the critical value J_{ab}^c is introduced. When J_{ab} is larger than this critical value, the interface

magnetism appears, and T_c for the system is higher than either T_c^a or T_c^b . When J_{ab} is smaller than the critical value, $T_c < T_c^a, T_c^b$.

Finally, we remark that the method is general and can be used to treat the ferromagnetic/antiferromagnet and antiferromagnet/antiferromagnet superlattices. With modifications in spatial fluctuations of the coupling J 's, the method can easily be generalized to superlattices involving certain type of amorphous magnetic materials.

Acknowledgments

This research was supported in part by the National Natural Science Foundation of China and US Office of Naval Research.

Figure captions

1. Unit cell of the superlattice composed of ferromagnetic materials A and B, where $L = L_a + L_b$ is the thickness of the cell. The solid and dashed lines represent the nearest-neighbor exchange coupling energies between spins in one material and in the interface, respectively.
2. Dependence of T_c on the thickness L . The interface coupling is chosen as $J_{ab} = 0.9 J_b$ and $J_a = 0.8 J_b$. Number of spin layers of material A is (a) 3, (b) 4 and (c) 5, (d) 6.
3. T_c as a function of L for $L_a = 3$ and $J_a = J_b$ but various interface coupling strengths. (a) $J_{ab} = 2.0 J_b$, (b) $J_{ab} = 1.46$ and (c) $J_{ab} = J_b$.
4. Same as Fig. 3 except that $J_a = 0.5 J_b$. (a) $J_{ab} = 3.0 J_b$, (b) $J_{ab} = 2.51 J_b$ and (c) $J_{ab} = 1.9 J_b$.
5. T_c as a function of L for $J_a = J_b$ but different J_{ab} and L_a . $J_{ab} = 2.0 J_b$ for curves a, b and c, and $J_{ab} = 0.1 J_b$ for a', b' and c'. The number of spin layers L_a is 3 for a, a', 5 for b, b', and 10 for c, c'.
6. Phase diagram in terms of the coupling J_{ab} and J_a for $L_a =$ (a) 3, (b) 4 and (c) 10.

References

1. H. R. Ma and C. H. Tasi, *Solid State Commun.* 55, 499 (1985).
2. J. Q. Zheng, J. B. Ketterson, C. M. Falco and I. K. Schuller, *J. Appl. Phys.* 53, 3150 (1982).
3. L. L. Hinchey and D. L. Mills, *Phys. Rev. B* 33, 3329 (1986).
4. L. L. Hinchey and D. L. Mills, *Phys. Rev. B* 34, 1689 (1986).
5. F. Fishman, F. Schwable and D. Schwenk, *Phys. Lett. A* 121, 192 (1987).
6. R. E. Camley and D. R. Tilley, *Phys. Rev. B* 37, 3413 (1988).
7. D. R. Tilley, *Solid State Commun.* 65, 657 (1988).
8. J. Barnaś, *J. Phys. C: Solid State Phys.* 21, 1021, 4097 (1988).
9. J. Barnaś, *J. Phys.: Condensed Matter* 2, 7173 (1990).
10. R. Monmura and T. Kaneyoshi, *J. Phys. C: Solid State Phys.* 12, 3979 (1979), *Z. Phys. B* 56, 307 (1984).
11. T. Hai and Z. Y. Li, *Phys. Stat. Solidi (b)* 156, 641 (1990).
12. H. B. Callen, *Phys. Lett.* 4, 161 (1963).

Fig. 1

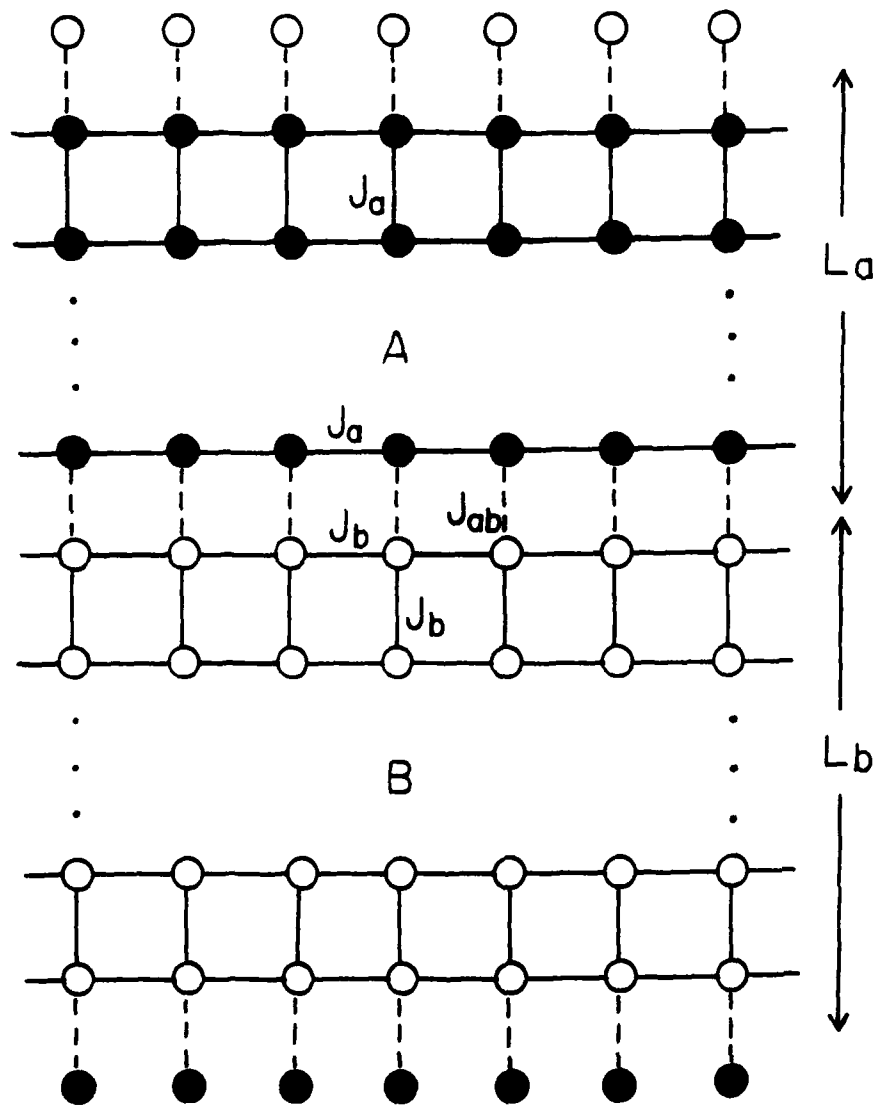


Fig. 2

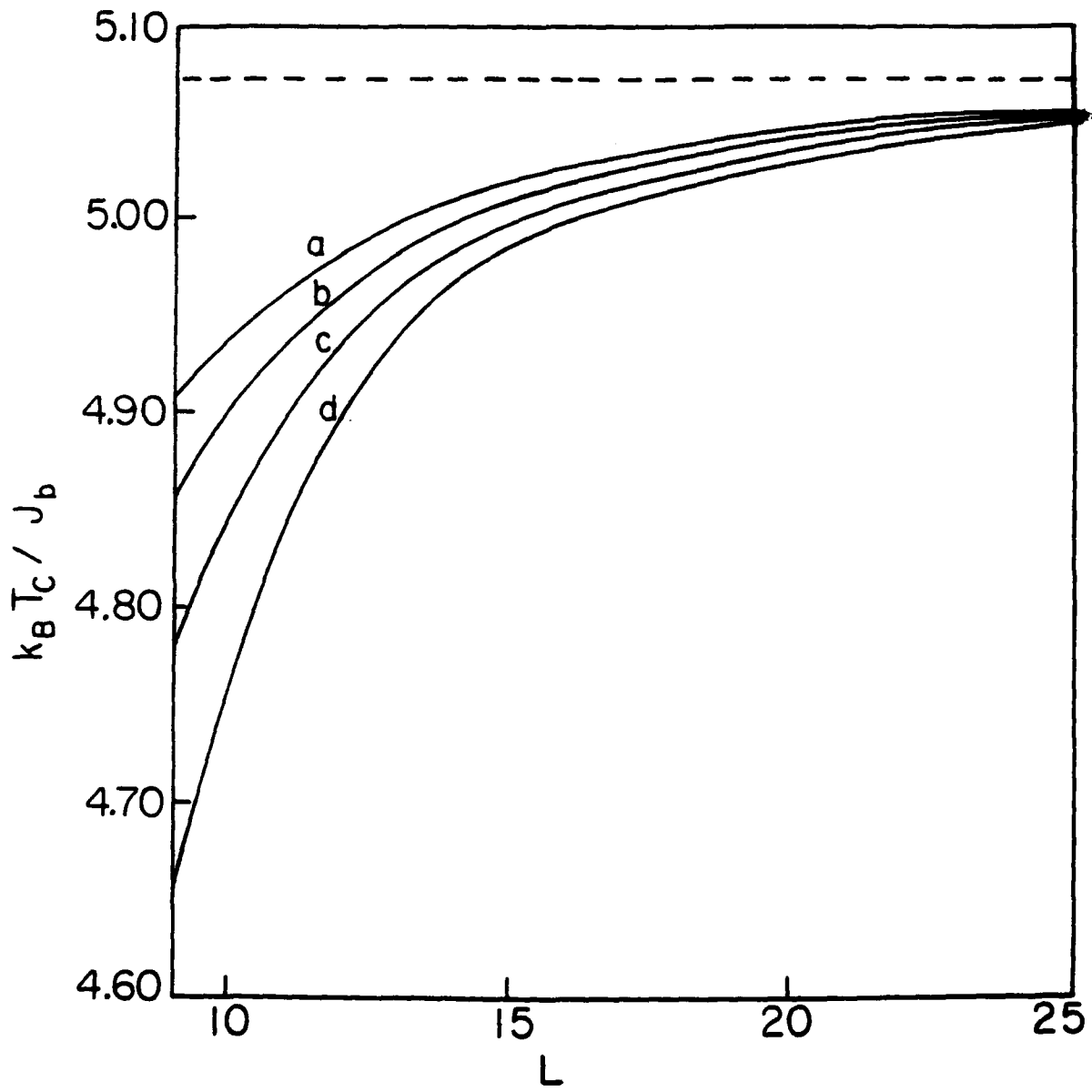


Fig 3

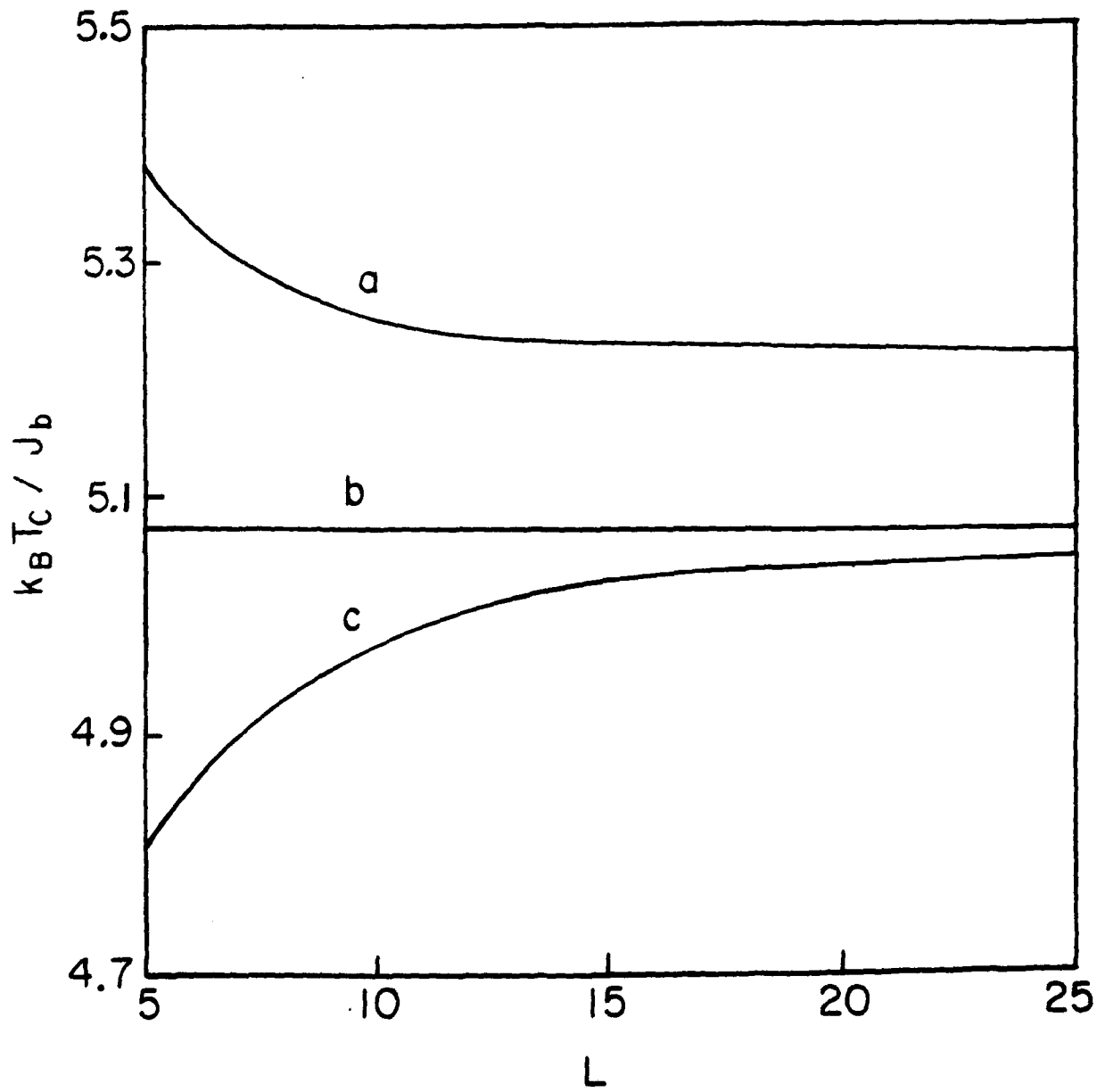


Fig. 4

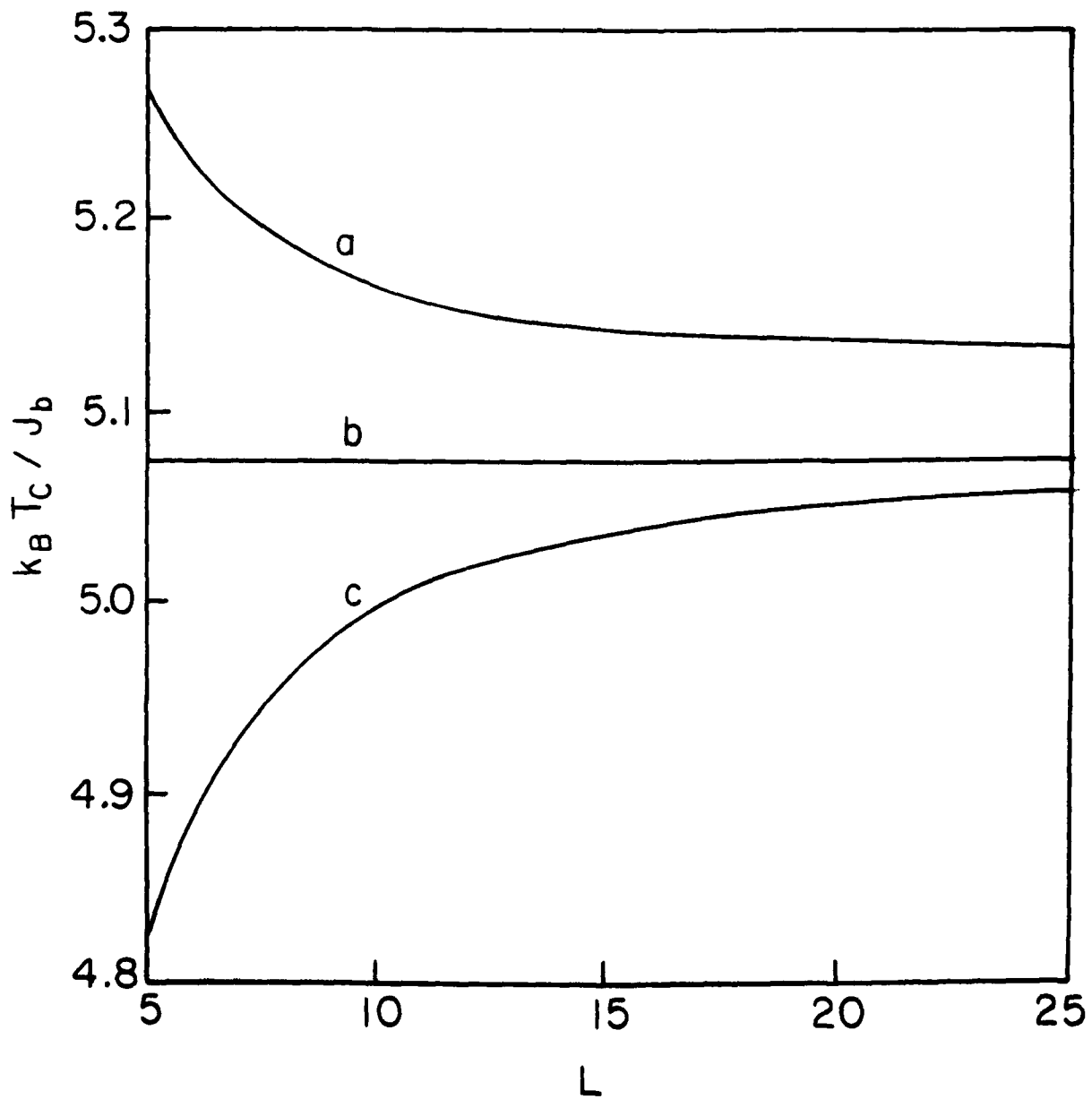


Fig. 5

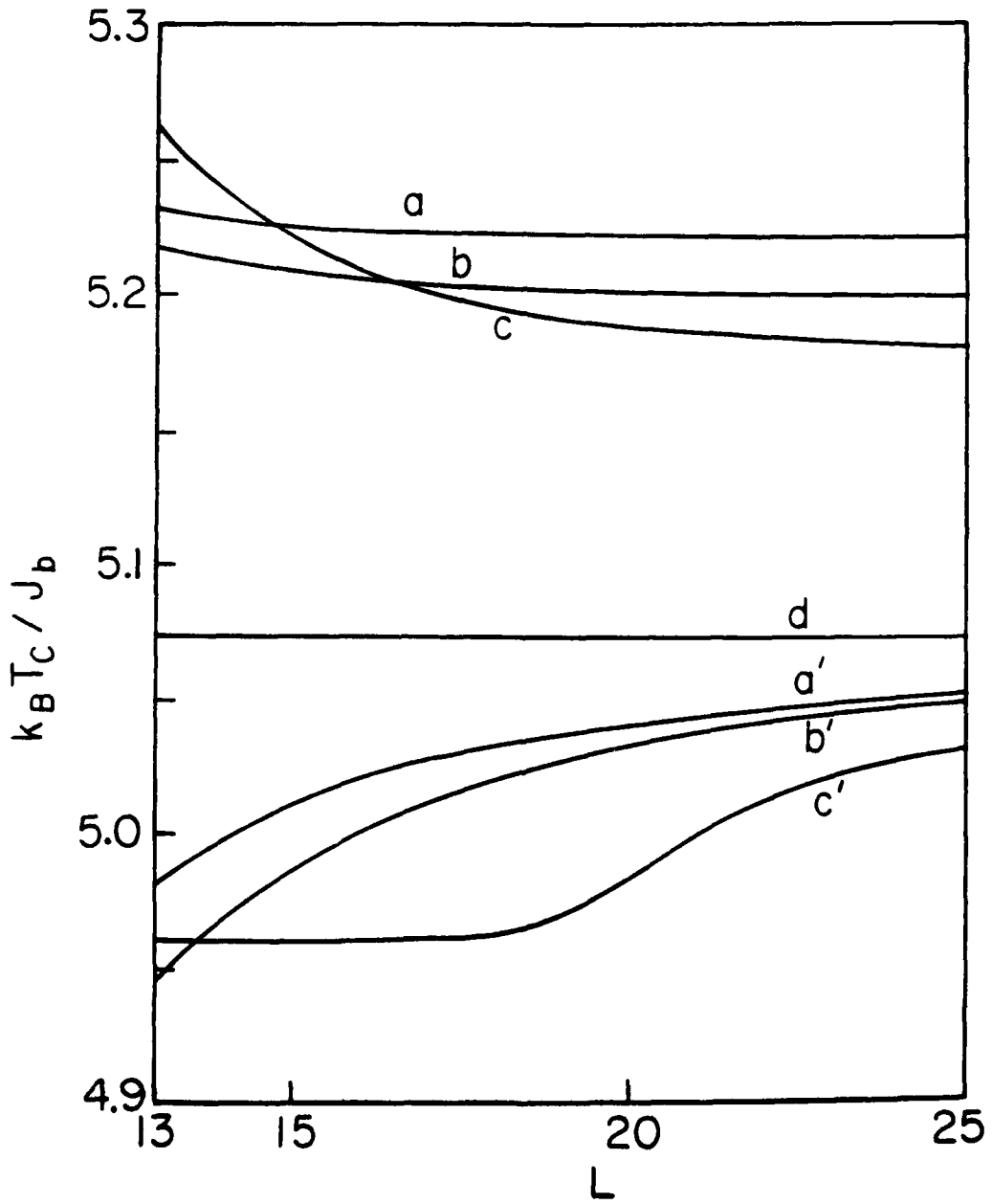
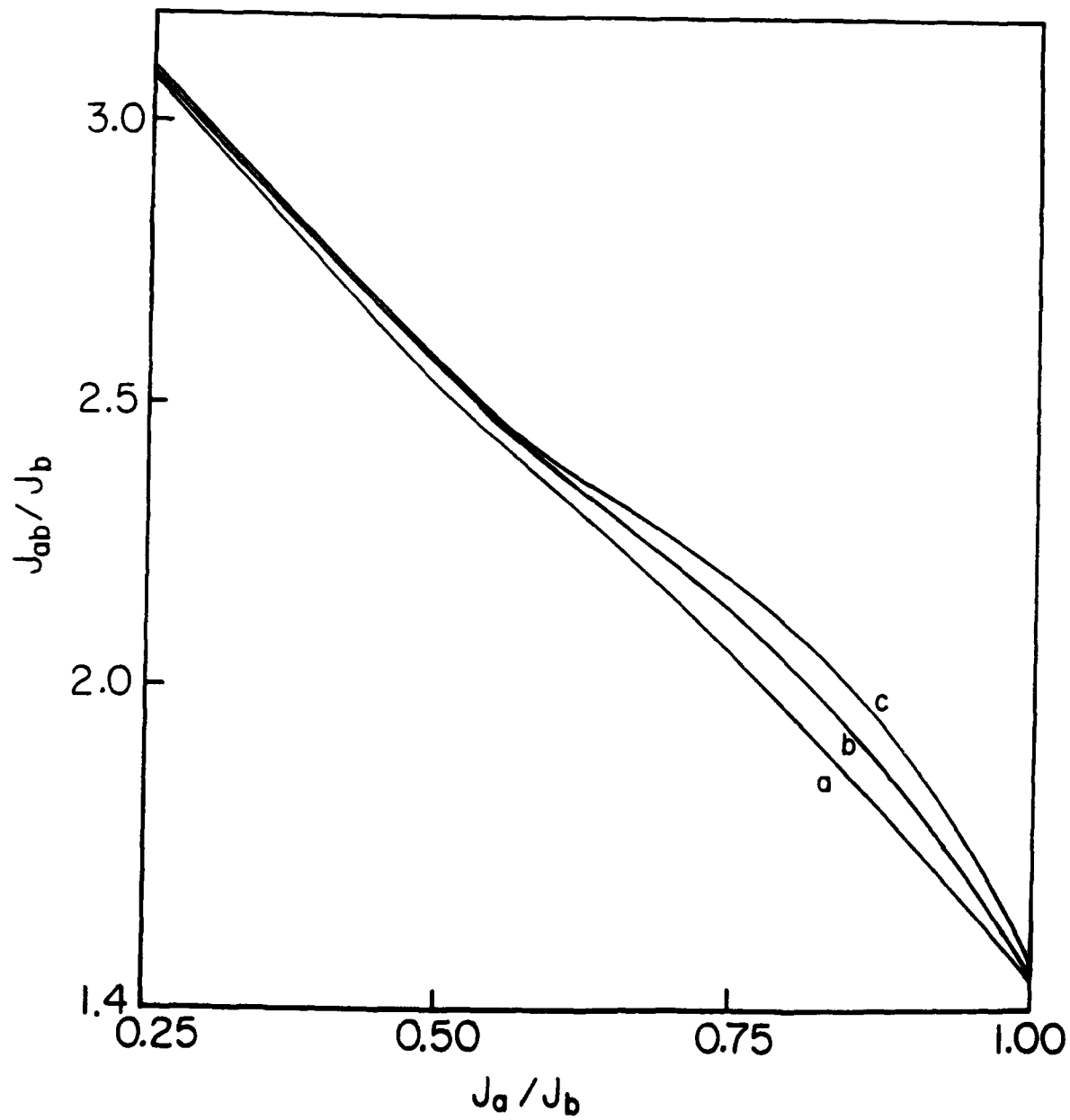


Fig. 6



Y90 Abstracts Distribution List for Solid State & Surface Chemistry

Professor John Baldeschwieler
Department of Chemistry
California Inst. of Technology
Pasadena, CA 91125

Professor John Eyler
Department of Chemistry
University of Florida
Gainesville, FL 32611

Dr. Sylvia Johnson
SRI International
333 Ravenswood Avenue
Menlo Park, CA 94025

Professor Paul Barbara
Department of Chemistry
University of Minnesota
Minneapolis, MN 55455-0431

Professor James Garvey
Department of Chemistry
State University of New York
Buffalo, NY 14214

Dr. Zakya Kafafi
Code 6551
Naval Research Laboratory
Washington, DC 20375-5000

Dr. Duncan Brown
Advanced Technology Materials
20-D Danury Rd.
New Milford, CT 06776

Professor Steven George
Department of Chemistry
Stanford University
Stanford, CA 94305

Professor Larry Kesmodel
Department of Physics
Indiana University
Bloomington, IN 47403

Professor Stanley Bruckenstein
Department of Chemistry
State University of New York
Buffalo, NY 14214

Professor Tom George
Dept. of Chemistry and Physics
State University of New York
Buffalo, NY 14260

Professor Max Lagally
Dept. Metal. & Min. Engineering
University of Wisconsin
Madison, WI 53706

Professor Carolyn Cassady
Department of Chemistry
Miami University
Oxford, OH 45056

Dr. Robert Hamers
IBM T.J. Watson Research Center
P.O. Box 218
Yorktown Heights, N Y 10598

Dr. Stephen Lieberman
Code 522
Naval Ocean Systems Center
San Diego, CA 92152

Professor R.P.H. Chang
Dept. Matls. Sci. & Engineering
Northwestern University
Evanston, IL 60208

Professor Charles Harris
Department of Chemistry
University of California
Berkeley, CA 94720

Professor M.C. Lin
Department of Chemistry
Emory University
Atlanta, GA 30322

Professor Frank DiSalvo
Department of Chemistry
Cornell University
Ithaca, NY 14853

Professor John Hemminger
Department of Chemistry
University of California
Irvine, CA 92717

Professor Fred McLafferty
Department of Chemistry
Cornell University
Ithaca, NY 14853-1301

Dr. James Duncan
Federal Systems Division
Eastman Kodak Company
Rochester, NY 14650-2156

Professor Leonard Interrante
Department of Chemistry
Rensselaer Polytechnic Institute
Troy, NY 12181

Professor Horia Metiu
Department of Chemistry
University of California
Santa Barbara, CA 93106

Professor Arthur Ellis
Department of Chemistry
University of Wisconsin
Madison, WI 53706

Professor Roald Hoffmann
Department of Chemistry
Cornell University
Ithaca, NY 14853

Professor Larry Miller
Department of Chemistry
University of Minnesota
Minneapolis, MN 55455-0431

Professor Mustafa El-Sayed
Department of Chemistry
University of California
Los Angeles, CA 90024

Professor Eugene Irene
Department of Chemistry
University of North Carolina
Chapel Hill, NC 27514

Professor George Morrison
Department of Chemistry
Cornell University
Ithaca, NY 14853

Best Available Copy

Professor Daniel Neumark
Department of Chemistry
University of California
Berkeley, CA 94720

Professor Robert Whetten
Department of Chemistry
University of California
Los Angeles, CA 90024

Professor David Ramaker
Department of Chemistry
George Washington University
Washington, DC 20052

Professor R. Stanley Williams
Department of Chemistry
University of California
Los Angeles, CA 90024

Dr. Gary Rubloff
IBM T.J. Watson Research Center
P.O. Box 218
Yorktown Heights, NY 10598

Professor Nicholas Winograd
Department of Chemistry
Pennsylvania State University
University Park, PA 16902

Professor Richard Smalley
Department of Chemistry
Rice University
P.O. Box 1892
Houston, TX 77251

Professor Aaron Wold
Department of Chemistry
Brown University
Providence, RI 02912

Professor Gerald Stringfellow
Dept. of Matls. Sci.
& Engineering
University of Utah
Salt Lake City, UT 84112

Professor Vicki Wysocki
Department of Chemistry
Virginia Commonwealth University
Richmond, VA 23284-2006

Professor Galen Stucky
Department of Chemistry
University of California
Santa Barbara, CA 93106

Professor John Yates
Department of Chemistry
University of Pittsburg
Pittsburg, PA 15260

Professor H. Tachikawa
Department of Chemistry
Jackson State University
Jackson, MI 39217-0510

Professor William Unertl
Lab. for Surface Sci.
& Technology
University of Maine
Orono, ME 04469

Dr. Terrell Vanderah
Code 3854
Naval Weapons Center
China Lake, CA 93555

Professor John Weaver
Dept. of Chem. Eng. & Mat. Sci.
University of Minnesota
Minneapolis, MN 55455

Professor Brad Weiner
Department of Chemistry
University of Puerto Rico
Rio Piedras, Puerto Rico 00931

Best Available Copy